PCCP

Accepted Manuscript

ROYAL SOCIETY OF CHEMISTRY

www.rsc.org/pccp

PCCP

ARTICLE

Surface- and tip-enhanced Raman scattering of bradykinin onto the colloidal suspended Ag surface

Received 21th April 2015,
Accepted 00th xxxx 20xx

DOI: 10.1039/x0xx00000x

www.rsc.org/

D. Swiech,[a] Y. Ozaki,[b] Y. Kim[c] and E. Proniewicz*[c]

In this paper, surface- (SERS) and tip-enhanced Raman scattering (TERS) techniques were used to determine the adsorption mode of bradykinin (BK), a small peptide implicated in; for example, carcinoma growth, onto colloidal suspended Ag surfaces under various environmental conditions, including: peptide concentrations (10^{-5} – 10^{-7} M), excitation wavelengths (514.5 and 785.0 nm), and pH of aqueous sol solutions (from pH = 3 to pH = 11). The metal surface plasmon and rheology of the colloidal suspended Ag surface were explored by ultraviolet-visible (UV-Vis) spectroscopy and atomic force/scanning electron microscope (AFM/SEM). The SERS results indicated that the peptide concentration of 10^{-5} M was the optimal peptide concentration for the monolayer colloidal coverage. The $Phe^{5/8}$ and Arg^{9} residues of BK generally participated in the interactions with the colloidal suspended Ag surfaces. The amide group appeared to be arranged in the same manner to the Ag surface in the pH range of 3 to 11. At acidic pH of the solution (pH = 3 to 5), the BK $–COO^-$ terminal group binds to the Ag surface as a bidentate (at pH = 3) or monodentate (at pH = 5) chelating ligand. At pH = 11, the imino group of Arg^{9}, probably due to its $–C=N^{\oplus}H_2$ protonation state, was not involved in the interaction with Ag. The reduction in the solution alkalinity (pH = 9) produced the deprotonation of the $–C=N^{\oplus}H_2$ group followed by the group rearrangement in a way favoring the interaction between the lone electrons pair on N and Ag. The TERS studies confirmed the proposed, on the basis of SERS, behavior of BK onto the colloidal suspended Ag at pH = 7 and showed that in different points of the colloidal suspended Ag surface the same peptide fragments approximately having the same orientations with respect to this surface interact with it.

Introduction

Bradykinin (BK) is an endogenous hormone peptide with the peptide sequence, Arg^{1}-Pro^{2}-Pro^{3}-Gly^{4}-Phe^{5}-Ser^{6}-Pro^{7}-Phe^{8}-Arg^{9}COOH (all amino acids are in the *L*-conformation).[1,2] This nanopeptide shows wide physiological and pathophysiological activities influencing the cellular and tissue responses.[3-5] For example, it is involved in the regulation of the blood pressure and smooth muscle contractions.[5-7] It increases the secretion of chloride ions by epithelial cells and endothelium prostaglandin secretion as well as induces sodium/water homeostasis.[8] Also, due to activation of the endothelial cells BK promotes dilatation of the vessel, vascular permeability, and reproduces characteristic four inflammation symptoms (heat, redness, swelling, and pain).[9,10] BK is also known as a factor of many diseases, such us: rhinitis, asthma, sepsis, rheumatoid arthritis, pancreatitis, epilepsy, and Alzheimer's disease.[10-12] It is suggested that BK is an important target for cancer growth; e.g., small-cell lung carcinoma (SCLC), non-SCLC, and prostate cancer.[13-15]

The conformational analysis of native BK by molecular spectroscopy methods[16-21] and computer simulations by molecular modeling methods[20,21] have revealed that BK mainly exists in a flexible random coil conformation in an aqueous solution and in a solid state. However, when BK binds to its B_1 and B_2 receptors, belonging to the hepthahelical transmembrane G-protein-coupled receptors (GPCRs),[22] or when exists in lipidic or micellar environment, that is a good model for the natural environment of BK when interacting with GPCRs, it changes structure from random coil to a bioactive predominantly β-turn structure (at the peptide *C*-terminus).[21,23-28] In this conformation the Phe residue of BK is shielded from aqueous environment.[25] Lopez et al., based on the solid-state NMR results, have also proposed that the *C*-terminal fragment (Ser^{6}-Arg^{9}) of BK, essential for the interaction with the B_2 receptor, adopts "distinct double-S-shaped structure".[28] Similarly, Kyle et al. by homology modeling and docking simulations have suggested a twisted S-shaped model of BK bound to the rat B_2 receptor, where Phe^{5}, Phe^{8}, and Pro^{7} of BK are bound in the hydrophobic cavities.[24] The removal of the BK *C*-terminal L-arginine (Arg^{9}), which drastically reduces the B_2 receptor affinity, has demonstrated that full-length BK is required for the B_2 receptor recognition and the receptor subtype selectivity depends on the presence of the charged terminal residues.[26,27]

In our laboratory, we also investigated several environmental and structural factors that may help to clarify the biological

[a] *Faculty of Foundry Engineering, AGH University of Science and Technology, ul. Reymonta 23, 30-059 Kraków, Poland. Email: proniewi@agh.edu.pl*
[b] *Department of Chemistry, School of Science and Technology, Kwansei Gakuin University, Gakuen 2-1, Sanda, Hyogo 669-1337, Japan.*
[c] *Department of Chemistry, Hankuk University of Foreign Studies, Yongin, Kyunggi-Do, 449-791, Korea.*
† Electronic Supplementary Information (ESI) available: See
DOI: 10.1039/x0xx00000x

behavior observed for bradykinin. We have reported surface-enhanced Raman scattering (SERS) results for BK and its Phe-D_5 isotopically labeled analogues deposited onto the roughened in the oxidation-reduction cycles Ag, Au, and Cu electrodes (at different applied electrode potential)[17,29] and onto the Au colloidal nanoparticles surface.[30] Briefly, our results have demonstrated that the Phe^5/Phe^8 residues (in tilted orientation of the rings) are mainly involved in the BK interaction with the colloidal Au surface with diameters of 20 nm and there is no preference of any of these two Phe residues to interact with the Ag, Au, and Cu surfaces. Together with the decrease of the Ag electrode charge successive reorientation of the Phe ring was detected, which was not observed in the case of the Au and Cu electrodes. Based on the results for specifically mutated BK analogues we have also designated Arg^9 to be the one which interacts with the colloidal Au surface and Ag, Au, and Cu electrodes.[31]

It is clear that the rheology of adsorbed species, at monolayer and submonolayer coverage, onto a metallic surface and the strength of competitive interaction of certain molecular fragments with this surface depend on analite concentration, pH of aqueous solution, nanostructure of a metallic surface, and hence on controlled distribution of the metal surface plasmon. This is why it is necessary to investigate the SERS effect for molecule at different experimental conditions. Thus, to delineate a complete picture of the metal/molecule interaction different types of metals and structured metal surfaces should be used. In the case of colloidal structured metal surfaces, the chemical method used for colloid preparation can be chose to obtain metal nanoparticle of proper size, shape, composition, morphology, and crystalline phase. The size and shape of these nanoparticles can be determined by SEM. Problem concerns only whether the SERS signal comes from molecules adsorbed on the surface of colloidal particles or from "hot spots". However, the measurements at different analyte concentrations and colloidal particles should resolve this problem. Using AFM coupled with Raman microscope simplifies measurement and gives clear results. For these reasons, we performed this type of research.

Thus, presented in this work SERS and TERS (tip-enhanced Raman scattering) research focuses on the rheology of the monolayer and submonolayer coverage of native BK onto colloidal suspended Ag surfaces under various environmental conditions, including peptide concentrations (10^{-5} – 10^{-7} M), excitation wavelengths (514.5 and 785.0 nm), and pH of aqueous colloidal solutions (from pH = 3 to pH = 11). Of note is the fact that there are only a limited number of TERS studies on biomolecules, including: nucleic acids,[32] viruses and bacteria,[33,34] lipids and human cell,[35] oxidised glutathione,[36] β-Amyloid(1–40) peptide fragments,[37] histidine,[38] di– (Tyr–Tyr and Phe–Phe) and tripeptides (Tyr–Tyr–Tyr), and bovine serum albumin[39].

SERS is the most common *in situ* technique in contexts involving determination of molecule structure, its orientation onto different metallic nanostructures, and complexation[17,40-44] because of its simplicity and ability to rapidly recognize the structures of peptides in aqueous solutions as well as its ability to probe different types of supramolecular architectures and to study the peptide-level adsorption phenomena at a metal/liquid interface. However, SERS is restricted by the relatively low spatial resolution. Thus, very important information about metal surface morphology cannot be obtained. Therefore, in the last several years, there is strong motivation to develop simple and rapid *in vitro*, or, if possible, *in vivo*, methods to study adsorption phenomena at the single-molecule level onto the nanostructure of the metallic surfaces with the controlled distribution of the metal surface plasmon. The TERS technique is believed to be one of such methods.[40,44-48] TERS combines Raman spectroscopy with scanning probe microscope (SPM) that collects images of metal surface using a physical probe that scans the specimen.[49] If a probe (tip) is coated with a SERS active metal, then the TERS effect occurs only within the immediate vicinity of the tip. Because the tip dimensions are typically <100 nm, the spatial resolution of this measurement would depend on the tip itself and would similarly be <100 nm.[50]

Experimental

Bradykinin synthesis

BK (powder, ≥98% (HPLC)) was purchased from Sigma-Aldrich (Poland).

UV-Vis measurements

The UV-Vis spectra of the aqueous Ag sol and BK/Ag sol system (measured after 15 minutes of mixing) (see Fig. 1) were recorded on a Shimadzu UV-3100 spectrophotometer.

Scanning electron microscope measurements

The SEM images of the aqueous Ag sol were recorded on a SEM instrument, model S-5000 (Hitachi Ltd., Japan), operated at 20 kV (see Fig. 1, Inset A).

Raman and SERS measurements in an Ag sol

Preparation of an aqueous Ag sol was carried out according to the following procedure.[51] Silver nitrate ($AgNO_3$) and sodium borohydride ($NaBH_4$) were purchased from Sigma-Aldrich and used without further purification. Three batches of the aqueous colloidal Ag solutions were prepared by the simple borohydride reduction of silver nitrate. Briefly, 42.5 mg of $AgNO_3$ dissolved in 50 mL of deionized water at 4 °C was added drop-wise to 150 mL of 2 mM $NaBH_4$ immersed in an ice bath, while the mixture was stirred vigorously. When the addition of $AgNO_3$ was completed, the resulting dark-yellow solution (pH = 7) was stirred continuously at 4 °C for approximately 1 h.

Aqueous BK solutions were prepared by dissolution of BK in deionized water (18 MΩ·cm). The normal pH value of the BK solution was around 7. The concentration of the sample was adjusted to 10^{-4} M prior to its being mixed with the colloid. Then, ten microliters of peptide sample was mixed with 20 μL of the Ag sol. To investigate the effect of pH, 0.1 and 0.05 M HCl and 0.1 and 0.05 M NaOH solutions were prepared and added to the peptide/colloid mixtures to obtain the desired pH. The mixture was kept for 15 min before the SERS measurement. The peptide solutions at different peptide concentrations (10^{-6} and 10^{-7}) were prepared by mixing the Ag colloidal solution (20 μl) and peptide solution (10 μl) diluted ten and hundred times.

The Raman and SERS spectra of BK were collected with Renishaw spectrometer (model inVia) operating in confocal mode

combined with a Peltier cooled CCD detector and a Leica microscope (50x long-distance objective). The 785.0 nm line of HP NIR diode laser (Invictus) and 514.5 nm line of Ar-ion laser (Renishaw) were used as excitation sources. The lasers power at the laser outputs was set at about 15 mW (SERS) and 20 mW (Raman). The typical exposure time for each the Raman and SERS measurement in this study was 40 s with four accumulations (series of 4 spectra, each accumulated 40 s = 160 s).

The SERS spectra were measured at eight spots on the surface of the colloidal Ag nanoparticles. The series of spectra were nearly identical (highly reproducible), except for small differences (up to 5%) in some band intensities.

TERS measurements on an Ag surface

Ten microliters of peptide sample was mixed with 20 µL of the Ag nanoparticles. After 15 minutes of incubation the mixture was deposited onto a glass plate and was dried in a vacuum dryer at 37°C for 30 minutes.

The TERS spectra were measured by an instrument consisting of a reflection-mode Raman microscope (Photon Design Inc.) equipped with a CCD detector (Princeton Instrument) and an AFM instrument (Photon Design, Nanostar NFRSM800). This system was arranged to introduce excitation light from the top of the sample and to collect backscattered signals using a 90x objective lens (numerical aperture, NA = 0.71). The 514.5 nm line from an Ar-ion laser (Spectra Physics, Stabilite 2017-06S) was used as the excitation source. The laser power at the sample point was 0.1 mW. A TERS needle coated with Ag (UNISOKU Co. Ltd.) was attached to the quartz tuning fork of a shear-force-based AFM at an angle of 45°. The tip radius of the probe was about 100 nm (spatial resolution of TERS experiments about 100 nm). The TERS tip approached the sample using the non-contact mode. A Raman signal was first collected under the tip-retracted conditions, and then, under the tip-approaed conditions at the same point. The typical exposure time for each Raman measurement was 20 s with eight accumulations (series of 10 spectra each of 20 s = 200 s) under the tip-retracted and tip-approached conditions. TERS spectra were calculated by subtracting a spectrum measured under the tip-retracted conditions from that collected under the tip-approached conditions.

Spectral analysis

The spectral analysis was performed using the GRAMS/AI 8.0 program (Thermo Scientific).

Second-derivative of SERS spectrum was calculated in the range of 1700 – 600 cm^{-1} using the Savitzky-Golay algorithm[52] that produces the least squares best fit of the data to the selected polynomial. The number of convolution points can range from 5 to 10,000, although values greater than the number of points across a peak is not normally used. Only odd numbers are used for number of convolution points and even values are rounded up. The number of convolution points and degree adopted in this work was set at 10 and 5, respectively. These parameters did not distort the spectra. However, a larger number of convolution points provided to the more smoothing result.

Results and discussion

Optical properties of Ag sol

The surface plasmon absorption, sizes, shape, and distribution of Ag nanoparticles were examined by the excitation spectra (UV-Vis) and scanning electron microscope (SEM)/atomic force microscope (AFM) images (Fig. 1). As is evident from Fig. 1, the Ag colloidal solution has the surface plasmon absorption maximum at 392 nm. The SEM/AFM images (Fig. 1A and 1B) point out that this unaggregated colloid contained the statistical Ag spheres with diameters of approximately 20 nm. The addition of BK (10 µL of 10^{-4} M) to the Ag colloid (20 µL) pronouncedly decreased the 392 nm band and caused a new band with the maximum at 500 nm. The aggregation produced large assemblies of apparently randomly adhering spheres, each of which with dimensions approximately equal to the original dimensions (Fig. 1C). These large assemblies

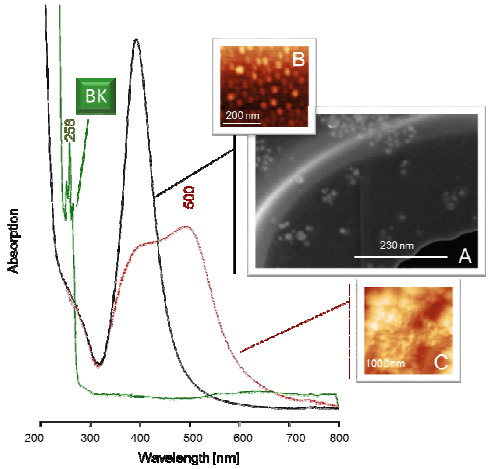

Fig. 1 The excitation (UV-Vis) spectra of BK in an aqueous solution (green line), an aqueous Ag sol (nanoparticles with diameter ~20 nm; black solid line), and BK/Ag sol system (brown dashed line) in the 200 – 800 nm range. Insets: the SEM (A) (20.0kV, x200K, scale 230 nm) and AFM (B) (scale 200 nm) images of the Ag colloidal nanoparticles and the AFM image of the peptide/Ag nanoparticles system (C) (scale 1000 nm).

are responsible for the color change (the metal particles become electronically coupled) that results from the broadness and red-shift to 500 nm of the plasmon resonance.

pH of the solutions, excitation wavelength, and peptide concentration dependent SERS measurements

By measuring the UV-Vis spectrum as a function of BK concentration, we observed that the maximum aggregation occurred at a concentration of 10^{-5} M. This value was used as the optimal peptide concentration for monolayer colloidal coverage.[53] The influence of the concentration of BK deposited onto the colloidal Ag surface in an aqueous solution at pH = 3 on the SERS spectrum is illustrated in Fig. 2. From this figure it is obvious that the BK SERS spectra for the peptide concentrations of 10^{-5} M, 10^{-6} M, and 10^{-7} M showed the same three pronounced spectral features (at 1396, 1239, and 1005 cm^{-1}) due to the carboxyl group, amide group(s), and Phe residue(s) vibrations (see Table 1 for detailed bands assignment). Although only in the SERS spectrum for the BK concentration of 10^{-5} M, the medium-weak 1589, 1575, 1449, and 1278 cm^{-1} bands due to Phe, the 1640 cm^{-1} allocated to the amide

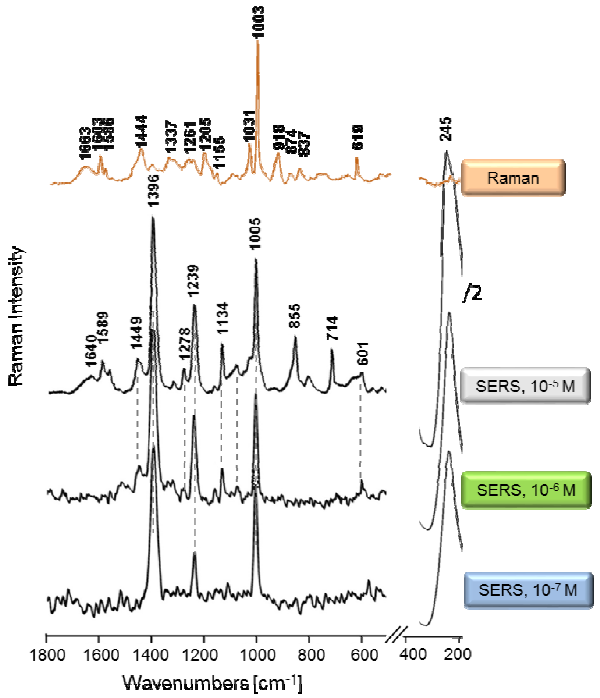

Fig. 2 The Raman spectrum of BK in the solid state and the SERS spectra of BK in the aqueous Ag sol (nanoparticles with diameter ~20 nm) at pH = 3 at different peptide concentrations: 10^{-5}, 10^{-6}, and 10^{-7} M. Measurement conditions: excitation wavelength: 785.0 nm; spectral range: 1800 – 500 cm^{-1}.

group, and the 1134, 855, and 714 cm^{-1} SERS signals assignable to Arg were observed.[17,29,41,54,55] These results suggest the model of peptide binding through the aforementioned peptide fragments within the investigated concentration range. However, some changes in the band intensities were noticeable according to peptide dilution from 10^{-5} M to 10^{-7} M. Namely, the relative intensities of the 1396 and 1239 cm^{-1} spectral features are comparable among the spectra for the peptide concentrations of 10^{-5} M and 10^{-6} M and are slightly stronger than those of 10^{-7} M. On the other hand, the intensity at 1005 cm^{-1} at the concentration of 10^{-7} M is equal to that at the concentration of 10^{-6} M and somewhat weaker than that of 10^{-5} M. However, neither the frequency shift nor the bandwidth alternations of these SERS signals were detected among the SERS spectra. This behavior indicates no reorientation of the aforementioned peptide fragments onto the colloidal suspended Ag surface upon the peptide dilution.

The SERS spectra of BK immobilized onto the colloidal Ag surface in aqueous solutions of pH = 3 and 7 obtained with the 785.0 and 514.5 nm laser excitations are presented in Fig. 3. It is noted that almost all bands observed in the SERS spectra excited with the 514.5 nm laser line (Fig. 3, traces: pH = 3 and 7, 785 nm) are also present in the spectra obtained upon the 785 nm laser excitation. However, the relative intensities of the bands in these spectra strongly depend on the excitation wavelength as is expected for resonance mechanism of enhancement. In general, the SERS spectra obtained with the 785.0 nm excitation wavelength are significantly strengthened compared to those obtained with the

Table 1 Wavenumbers and proposed band assignments for the Raman, SERS, and TERS spectra of BK adsorbed onto the Ag surfaces.

	Wavenumber [cm^{-1}]					
	Raman	SERS in an aqueous Ag sol 785.0 nm 10^{-5} M		probing point no. 1		
		pH 3	pH 7	SERS	TERS	2'nd deriv.
Amide I and/or Arg [ν_{as}(C=N)]	1663	1640	1643	–	1645	1664
Phe [ν_{8a}]	1603	1589	1603	1601	–	–
Phe [ν_{8b}]	1586	1575	1586	1565	1584	1581
Am II, Arg [δ(NH)], and/or Arg [$\nu_{as}(COO^-)$]	–	–	–	–	1537	1537
Phe [ν_{19a}] and/or Arg [ν_s(C=N)]	1492	–	–	–	1500	1506
Phe [ν_{19b}] and/or Arg [δ(NH)]	1444	1449	1448	–	1450	1450
Arg [$\nu_s(COO^-)$]	1408	1396	–	–	–	–
Arg [$\rho_w(CH_2)$ and ν(C–N)]	–	–	–	1369	1366	1366
Arg [$\rho_w(CH_2)$]	1337	1318	–	1327	1317	1324
Phe [ν_3]	1261	1278	1277	1277	1278	1278
Amide III	1246	1239	1253	–	1225	1226
Phe [ν_{7a}]	1205	–	1205	–	–	–
Phe [ν_{9a}] and/or Arg [δ(NH)]	–	1161	1181	–	1199	1195
Arg [δ(NH)] and/or ν_{as}(CNC)	1155	1134	1155	–	1154	1154
Arg [δ(NH)]	–	–	–	–	1122	1119
Arg [ν_s(C–C) + ν(C–N)]	1090	1079	1075	1085	1089	1087
Phe [ν_{18a}]	1031	1034	1032	–	–	1030
Phe [ν_{12}]	1003	1005	1004	1001	1001	1001
ν_{as}(CCC) + Phe [ρ_{oopw}(CH)]	–	–	–	–	962	959
ν(C–C), ν(C–N), and/or Arg [δ(CH_2)]	918	923	924	913	918	920
Arg [$\rho_r(CH_2)$]	874	870	876	–	893	899
Arg [δ(NH)]	837	–	846	810	–	808
Arg [δ(NH)]	–	–	764	764	765	765
Arg [$\rho_r(CH_2)$]	–	714	–	701	699	699
Arg [$\rho_w(CH_2)$]	658	–	–	670	674	674
Amide	–	–	–	648	649	645
Phe [ν_{6b}]	619	622	622	616	618	618
ν(Ag–N)	–	–	380	380	380	–
ν(Ag–O)	–	245	–	–	–	–
ν(Ag–N)	–	–	230	230	230	–

Abbreviations: ν – stretching, ν_s and ν_{as} – symmetric and asymmetric, respectively, stretching, δ - deformation, ρ_w – wagging, and ρ_r – rocking vibrations; Arg – L-arginine and Phe – L-phenylalanine

514.5 nm laser excitation. This has to be associated with existing vibrational coupling often associated with the intervention of charge-transfer transition that was discussed in detail by Birke and Lombardi.[56] Although there is no evidence of a charge-transfer transition in the UV-Vis spectrum (Fig. 1). At this peptide concentration (10^{-5} M), investigated molecules form a monolayer at

most. Thus, this thin layer will result in a weak charge-transfer transition, which would be most likely overwhelmed by the tail of UV-Vis coagulation peak. That is why it is not clearly observed in the UV-Vis spectrum.

As mentioned in the above paragraph, the BK SERS spectrum at pH = 3 upon the 785.0 nm excitation line (Fig. 3, the second trace from the bottom) is dominated by the 1396, 1239, and 1005 cm^{-1} bands due to the carboxyl group, amide group(s), and Phe residue(s) vibrations that are accompanied by other SERS signals of these molecular fragments (see Table 1). The models of the backbone structure of BK bound to the human B_2 receptor, given by Lopez at al.,[28] follow that $Phe^{5/8}$ and $Arg^{9}COO^{-}$ in the BK chain were those residues that interact with the colloidal suspended Ag surface and maintain the rather rigid structure of BK *C*-terminus. This is in agreement with the biological activity studies (see Introduction) that have demonstrated that the *C*-terminal fragment of BK is essential for the interaction with the B_2 receptor. Based on the amide bands positions (1640 and 1239 cm^{-1}) this structure seems to correspond to the β-turn conformation. Again, this is in line with studies of the biological activity, which indicate that BK adopts this structure when binds to GPCRs (see Introduction).

The weaker 1005 cm^{-1} band in the discussed SERS spectrum (Fig. 3, the second trace from the bottom) in comparison to that in the corresponding Raman spectrum indicates that the Phe ring adopted a more or less tilted orientation with respect to the colloidal suspended Ag surface. The higher wavenumber (by 3 cm^{-1}) and band width (by 6 cm^{-1}) of the 1005 cm^{-1} SERS signal in comparison to those in the Raman spectrum support the above statement. This proposed orientation of Phe corresponds to its behaviour in an aqueous colloidal Au sol.[30] On the other hand, the strong enhancement of the 1396 cm^{-1} spectral feature (fwhm = 20 cm^{-1}; fwhm – full width at half maximum), that is weakly scattered at ~1405 cm^{-1} (fwhm = 14 cm^{-1}) in the BK Raman spectrum, leads to the conclusion that the *C*-terminal deprotonated carbonyl moiety (pK_{a1} = 1.8) remained in close contact with the surface of colloidal Ag at pH = 3 in a manner that favors the interaction of the lone pair of electrons on oxygen('s) with this surface. The 1520 cm^{-1} band in the BK SERS spectrum at pH = 3 upon the 514.5 nm irradiation due

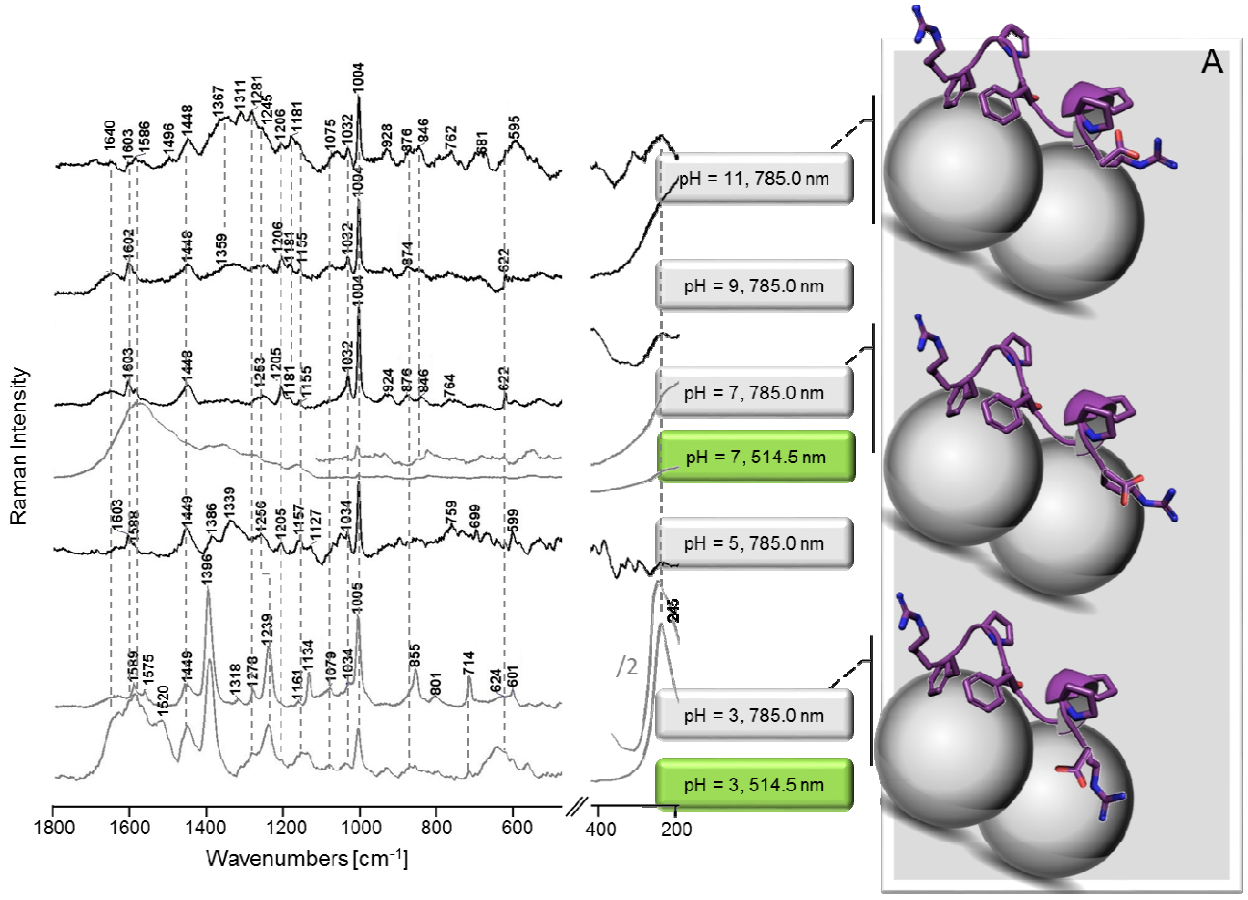

Fig. 3 The SERS spectra of BK in the aqueous Ag sol (nanoparticles with diameter ~20 nm) at different pH of solution and excitation wavelengths. Measurement conditions: peptide concentration: 10^{-5} M; excitation wavelengths: 785.0 and 514.5 nm; pH values between 3 and 11; spectral range: 1800 – 200 cm^{-1}. Inset A: proposed adsorption modes of BK at different pH of solutions.

to antisymmetric stretching vibrations of the –COO^- group confirms the –COO^-···Ag interactions and sheds some light on a carboxylate-binding mode. This is because the wavenumberts of the antisymmetric ($\nu_{as}(COO^-)$) and symmetric ($\nu_s(COO^-)$) stretching vibrations of the carboxylate group have been shown to be indicative of the strength of coordination and the mode of binding in the carboxylate compounds, which can be monodentate or bidentate.[57] The carboxylate group has the C_{2v} point symmetry group when acts as a bidentate chelating ligand. In such case, the wavenumbers of –COO^- are expected to be similar as those seen in the free ion spectrum. Although coordination to a heavy metal atom may cause shift in these wavenumbers, these changes are small.[58] On the other hand, for the monodentate coordination the carboxylate ligand shows a lower symmetry than that of the bidentate form and therefore should exhibit similarities to the spectrum of the monomeric undissociated carboxylic acid itself. For monodentate carboxylate bonding it has been reported that $\nu_{as}(COO^-)$ increases, whereas $\nu_s(COO^-)$ decreases in wavenumbers and the frequencies of these modes should differ by 105 – 140 cm^{-1}.[59] Based on the above and on the noticed 124 and 154 cm^{-1} separations in the wavenumbers of the carboxylate group vibrations at pH = 3 and 5, respectively, it seems that in an aqueous solution at pH = 3 the BK –COO^- terminal moiety binds to the Ag nanoparticles surface through the both oxygen atoms of the carboxylate group, whereas at pH = 5 the carboxylate moiety serves rather as the monodentate chelating ligand.

Fig. 3 presents the pH-dependent changes (from pH = 3 to pH = 11) in the SERS profile of BK adsorbed onto the Ag nanoparticles in an aqueous solution at the concentration of 10^{-5} M. An examination of this figure showed that the SERS spectra at pH = 5 and greater pH levels, in contrast to the previously discussed SERS spectrum of BK at the pH solution of 3 (Fig. 3, trace: pH = 3, 785.0 nm), have very similar spectral patterns and consist of bands mainly due to the Phe ring modes, including: ν_{12} (1004 cm^{-1}), ν_{18a} (1032 cm^{-1}), ν_{9a} (1181 cm^{-1}), ν_{7a} (1206 cm^{-1}), ν_3 (1281 cm^{-1}), $\nu_{19b/19a}$ (1448/1496 cm^{-1}), and $\nu_{8b/8a}$ (1586/1603 cm^{-1}), to the amide bond modes (1640 and ~1245 cm^{-1}), and to the Arg side-chain modes (δ(NH) at 1448, 1181, 1155, and 846 cm^{-1}; $\rho_{w/r}(CH_2)$ at 1367, 1311, and 876 cm^{-1}; and ν_s(C–C) + ν(C–N) at 1075 cm^{-1}).[17,29,41,54,55]

The aforementioned SERS signals indicate that the Phe[5/8] and Arg[9] residues interacted with the colloidal Ag surface at the pH range from 5 to 11. However, these individual bands have different relative intensities because of the differences in the strength of the interactions between Phe[5/8] and Arg[9] and the substrate. The relative intensity changes in the SERS spectra upon the decrease of the solution acidity were connected mainly with the –CH_2– deformations ($\rho_{w/r}(CH_2)$) and –C=NH oscillations (ν(C=N)) of the Arg[9] side-chain and with the ν_{12} mode of Phe[8]. Thus, the amide bond appeared to be located sufficiently close in the same manner to the Ag surface at any pH of solutions. The bands of the $\rho_{w/r}(CH_2)$ modes decreased in the relative intensity when the pH of solution becomes more acidic because either slight weakening of the interactions between the –CH_2– group(s) of Arg[9] and the Ag colloidal surface occurred or the Arg[9] aliphatic chain laid on this surface when the pH of solutions changed from basic to acidic. At pH = 7, the SERS signal of the ν_{12} mode weakened with respect to that at pH = 3 and 5. This

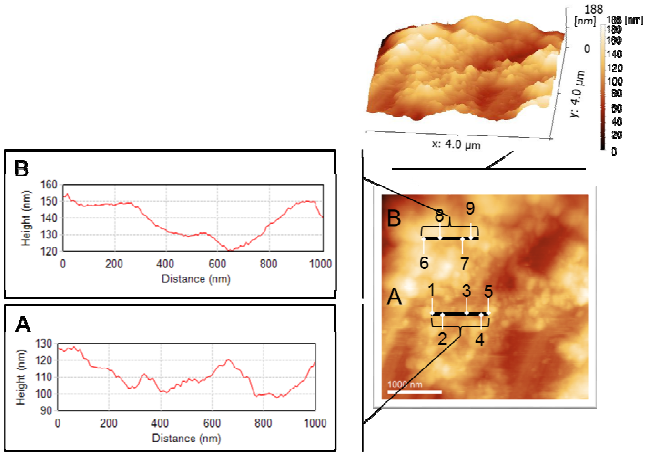

Fig. 4 The AFM image of the BK/Ag sol system (scale bar 1000 nm) with the nine probing spots where the TERS spectra were collected and the surface characteristic diagrams: A (for points from A1 to A5) and B (for points from B6 to B9).

phenomenon implies that at this pH the Phe ring tilted towards the substrate. On the other hand, the weak intensity of the 1640 cm^{-1} band at pH = 11 indicates that the lone electrons pair on nitrogen of the Arg[9] –C=NH group was not involved in the interaction with Ag at this pH, probably due to the protonation state of this group (the presence of –C=$N^{\oplus}H_2$, pK=12; pK values depend on temperature, ionic strength, and the microenvironment of the ionizable group). The decrease in pH from 11 to 9 has caused deprotonation of the –C=$N^{\oplus}H_2$ group followed by the group rearrangement in a way favoring the interaction between the lone electrons pair on N and Ag. Additionally, at the lowest two pH of solutions, the new band (at 1386 cm^{-1} at pH = 5 and at 1396 cm^{-1} at pH = 3) due to the carboxylate group vibrations appeared. This band is weak at pH = 5, whereas it is the strongest SERS signal in the spectrum at pH = 3. Consequently, this suggests that, at the pH solutions level ranging from 11 to 7 there is no contact between the carboxylate group of the terminal Arg residues and the Ag surface. Although at pH = 5, the –COO^- moiety assisted in the BK···Ag interaction, whereas at pH = 3 it strongly binds to the Ag nanoparticles surface.

The SERS spectra of BK in an aqueous solution at pH = 3 (Figs. 3 and 4) show also the strong 245 cm^{-1} band due to the Ag–O stretching vibrations,[60-62] whereas the BK SERS spectrum at pH = 5 has the ν(Ag–O) mode exhibiting only the weak intensity. Thus, these phenomena support the earliest statements that at pH = 3 only, the strong interaction between both oxygen atoms of the carboxylate group and the Ag surface occurred. At pH = 7 in the SERS and TERS spectra the weak 230 and 382 cm^{-1} spectral features, assignable to the Ag–N stretching vibrations, appear.[60] These SERS signals infer the formation of the Ag-N bond, which can be confirmed by the enhancement of the 1369 cm^{-1} band ($\rho_w(CH)_2$+ν(CN)).

TERS measurements

Fig. 4 presents the AFM image of the contact Ag surface (scale bar 1000 nm) with the nine randomly chosen probing points where the TERS spectra were measured and the surface characteristic diagrams: A (for points from A1 to A5) and B (for points from B6 to B9). As is evident from this figure, colloid drying produced the Ag film with randomly distributed different-sized aggregates (high up to ~50 nm, length 80 – 500 nm) of the 20 nm spherical Ag nanoparticles. For the nine probing points, Fig. 5 shows the TERS spectra measured under the tip-approached conditions. Fig. 5 also presents the TERS spectrum (red dashed line) collected under the tip-retracted conditions at the probing point no. A1. The comparison of the BK spectra at the A1 point evidences the same set of bands; however, the TERS signals are significantly enhanced in comparison to those in the SERS spectra. To enhance resolution of the spectrum measured under tip-approached conditions at the A1 probing point (complex spectrum containing overlapped bands) the second-derivative (in the range 1700 – 600 cm^{-1}) spectrum was calculated (Fig. 5A). Also, a TERS spectrum was calculated (Fig. 5B) by subtracting the spectrum collected under the tip-retracted conditions from that measured under the tip-approached conditions. In general, there is good agreement between the read and calculated bands positions (Table 1). The TERS wavenumbers (the 1645, 1584, 1537, 1500, 1366, 1317, 1278, 1225, 1199, 1122, 1089, 1001, 962, 699, and 624 cm^{-1}) (Fig. 6B) demonstrated also close similarity to the bands frequencies in the SERS spectra of BK in an aqueous Ag silver sol (Fig. 3). Therefore, the TERS spectra support predicted mode of BK adsorption, through Phe[5/8] and Arg[9], drown based on the SERS spectra. However, there are some changes in the bands relative intensities among the TERS spectra recorded at the different probing points. These changes are mainly caused by molecules adsorbed onto the heterogeneous colloidal suspended Ag surface (the changes in the morphology of the surface presents the diagram A and B) (see Fig. 4) than by molecules adsorbed on "hot spots". The main difference denotes to the strong broad band with maximum centered at 912 cm^{-1}, due to superposition of the ν(C–C) + ν(C–N) (~899 cm^{-1}), δ(CH_2) (~920 cm^{-1}), and ν_{as}(CCC) + $\rho_{oopw}(CH)_{Phe}$ (~950 cm^{-1}) modes, in the TERS spectra at the A probing spots.

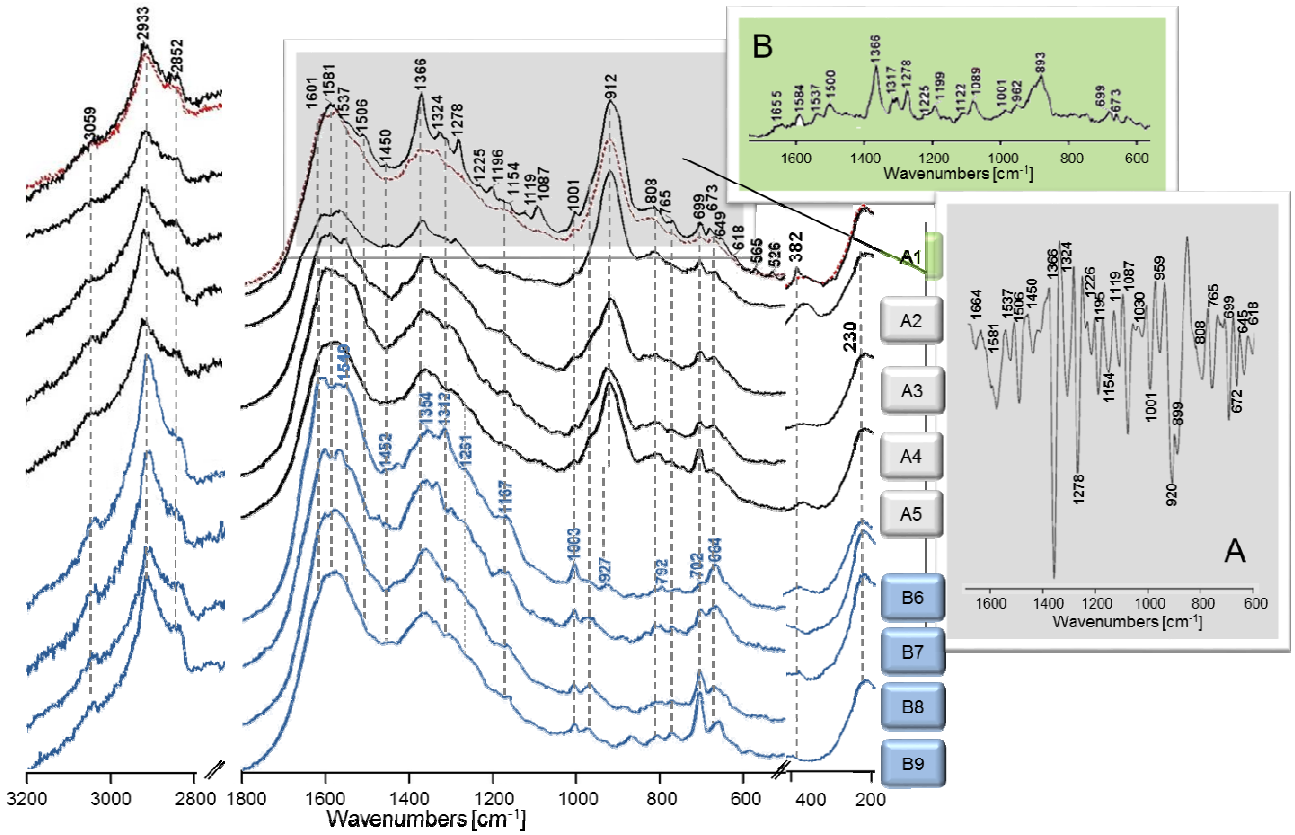

Fig. 5 The SERS (red dashed line; at sampling point no. A1) and TERS spectra measured upon tip-approached conditions (black (at A sampling points) and blue (at B sampling points) solid lines) of BK adsorbed onto the Ag nanoparticles. Measurement conditions: peptide concentration: 10^{-5} M; pH = 7; excitation wavelength: 514.5 nm; spectral range: 3200 – 2800 and 1800 – 500 cm^{-1}. Insets: the second-derivative TERS spectrum (A) and the TERS spectrum obtained by subtracting the spectrum collected upon tip-retracted conditions from that measured upon tip-approached conditions at the A1 sampling point (B).

A noteworthy fact is that the strong and broad 1210 – 1450 and 1450 – 1580 cm^{-1} TERS bands due to the 'D peak' and 'G peak', respectively, of the hydrogenated amorphous carbon contamination, which is formed on a metal surface during rapid photodecomposition (by the highly enhanced electromagnetic field in the "hot" tip-sample nanogap) of the adsorbed organic compound influence the TERS spectra.[63-66]

Conclusions

The adsorption mode of BK onto the colloidal Ag surfaces (with statistical Ag nanoparticle diameters of 20 nm) and the changes of this mode, which are influenced by peptide concentrations (10^{-5} – 10^{-7} M), excitation wavelengths (514.5 and 785.0 nm), and pH levels of the aqueous sol solutions (from pH = 3 to pH = 11), were determined by SERS. The TERS studies of BK behavior onto the colloidal suspended Ag surface were also carried out and the results were compared with the corresponding SERS and Raman, of bulk BK, data. By observing the spectral profiles, the following conclusions were drawn:

i)The BK concentration of 10^{-5} M was the optimal peptide concentration for monolayer colloidal coverage.

ii)The relative intensities of the SERS bands in the spectra strongly depend on the excitation wavelength as is expected for resonance mechanism of enhancement.

iii)The $Phe^{5/8}$ and Arg^{9} fragments of BK generally participated in the interactions with the colloidal suspended Ag nanoparticles. This result together with the earlier data indicates that BK shows similar mode of adsorption onto different nanostructured Ag, Au, and Cu surfaces[21,32,33] and the same molecular fragments are responsible for both the metal binding and receptor binding (see Introduction).

iv)With the change of pH of the colloidal Ag solution from 3 to 11, distinct change in the protonation state of BK adsorbed onto the Ag colloidal surface was observed, which was clearly evident in the reorientation of the $Phe^{5/8}$ and $Arg^{9}COO^{-}$ onto the Ag surface.

v)The TERS studies of BK showed that the bands of the same peptide fragments approximately having the same orientations with respect the colloidal suspended Ag film, with randomly distributed different-sized aggregates (high up to ~50 nm, length 80 – 500 nm) of the 20 nm spherical Ag nanoparticles, arise from the different probing points onto the Ag film.

vi)The TERS experiments demonstrated clearly the feasibility of the TERS technique for studying complex biological molecules.

Conflict of Interests

The authors have no conflict of interests to declare.

Acknowledgments

This work was supported by the National Research Center of the Polish Ministry of Science and Higher Education (Grant No. N N204 354840 to E.P. and Grant No. 2012/05/N/ST4/00175 to D.Ś.). We thanks to Prof. C. Glaubitz (Department of Biophysical Chemistry, Goethe University, Frankfurt am Main, Germany) for the low energy model structure of BK bound to the human B_2 receptor.

Notes and references

1 J. M. J. M. Stewart, L. Gera, E. J. York, D. C. Chan and P. A. Bunn Jr., in *Peptides 2000*, ed. J. Martinez and J. A. Fehrentz, EDK, Paris, 2001, pp. 637.
2 D. J. Campbell, in *Handbook of Biologically Active Peptides*, ed. A. J. Kastin, Academic Press, Elsevier, San Diego, 2006, pp. 1175.
3 O. Zaika, M. Mamenko, R. G. O'Neil and O. Pochynyuk, *Am. J. Physiol. Renal. Physiol*., 2011, **300**, F1105.
4 M. E. Moreau, N. Garbacki, G. Molinaro, N. J. Brown, F. Marceau and A. Adam, *J. Pharmacol. Sci.,* 2005, **99**, 6.
5 F. Marceau, J. F. Hess and D. F. Bachvarov, *Pharmacol. Rev*., 1998, **50**, 357.
6 R. Bhoola, R. Ramsaroop, S. Naidoo, W. Muller-Esterl and K. D. Bhoola, *Immunopharmacology*, 1997, **36**, 161.
7 W. Xiong, J. Chao and L. Chao, *Hypertension,* 1995, **25**, 715.
8 J. Sadowski and B. Badzynska, *J. Physiol. Pharmacol*., 2008, ***59*** Suppl. ***9***, 105.
9 L. M. F. Leeb-Lundberg, F. Marceau, W. Müller-Esterl, D. J. Pettibone and B. L. Zuraw, *Mol. Pharmacol*., 2007, **71**, 494.
10 M. Maurer, M. Bader, M. Bas, F. Bossi, M. Cicardi, M. Cugno, P. Howarth, A. Kaplan, G. Kojda, F. Leeb-Lundberg, J. Lötvall and M. Magerl, *Allergy,* 2011, **66**, 1397.
11 F. Marceau and D. Regoli, *Nat. Rev. Drug Discov*., 2004, **3**, 845.
12 J. B. Calixto, D. A. Cabrini, J. Ferreira and M. M. Campos, *Pain,* 2000, **87**, 1.
13 J. M. Stewart, *Curr. Pharm. Design,* 2003, **9,** 2036.
14 J. S. Taub, R. Guo, L. M. Leeb-Lundberg, J. F. Madden and Y. Daaka, *Cancer Res*., 2003, **63**, 2037.
15 B. A. Teicher, *Biochem. Pharmacol.* 2014, **87**, 211.
16 J. W. Fox, R. J. Vavrek, A. T. Tu and J. M. Stewart, *Peptides,* 1982, **1**, 193.
17 E. Proniewicz, D. Skołuba, I. Ignatjev, G. Niaura, D. Sobolewski, A. Prahl and L. M. Proniewicz, *J. Raman Spectrosc.,* 2013, **44**, 655.
18 L. Denys, A. A. Bothner-By, G. H. Fisher and J. W. Ryan, *Biochemistry,* 1982, **21**, 6531.
19 G. Kotovych, J. R. Cann, J. M. Stewart, H. Yamamoto, *Biochem. Cell Biol.* **1998**, *76*, 257.
20 C. Bonechi, S. Ristori, G. Martini, S. Martini and C. Rossi, *Biochim. Biophys. Acta,* 2009, **1788**, 708.
21 M. Manna and C. Mukohopadhyay, *Langmuir,* 2011, **27**, 3713.
22 J. F. Hess, J. A. Borkowski, J. S. Young, C. D. Strader and R. W. Ransom, *Biochem. Biophys. Res. Commun*., 1992, **184**, 260.
23 G. Kotovych, J. R. Cann, J. M. Stewart and H. Yamamoto, *Biochem. Cell Biol.*, 1998, **76**, 257.
24 D. J. Kyle, S. Chakravarty, J.A. Sinsko and T. M. Stormann, *J. Med. Chem.,* 1994, **37**, 1347.
25 Ch. Chatterjee and Ch. Mukhopadhyay, *Biochem. Biophys. Research Com*., 2004, **315**, 866.
26 R. F. Turchiello, M. T. Lamy-Freund, I. Y. Hirata, L. Juliano and A. S. Ito, *Biopolymers,* 2002, **65**, 336.
27 M. Pellegrini, P. Tancredi, D. F. Rovero and J. Mierke, *J. Med.Chem.,* 1999, **42**, 3369.
28 J. J. Lopez, A. K. Shukla, C. Reinhart, H. Schwalbe, H. Michel and C. Glaubitz, *Angew. Chem. Int. Ed.,* 2008, **47**, 1668.
29 E. Proniewicz, I. Ignatjev, G. Niaura, D. Sobolewski, A. Prahl and L.M. Proniewicz, *J. Raman Spectrosc.*, 2013, **44**, 1096.
30 D. Skołuba, D. Sobolewski, A. Prahl and E. Proniewicz, *Spectrosc-Int J.,* 2014, 1.
31 D. Sobolewski, E. Proniewicz, D. Skołuba, A. Prahl, Y. Ozaki, Y. Kimd and L. M. Proniewicz, *J. Raman Spectrosc*. 2013, 44, 212.
32 A. Rasmussen and V. Deckert, *J. Raman Spectrosc.,* 2006, **37**, 311.
33 P. Hermann, A. Hermelink, V. Lausch, G. Holland, L. Möller, N. Bannert and D. Naumann, *Analyst***,** 2011,**136**, 1148-1152.

34 T. Schmid, A. Messmer, B.-S. Yeo, W. Zhang and R. Zenobi, *Anal. Bioanal.Chem.* 2008, 391, 1907.
35 R. Bohme, M. Richter, D. Cialla, P. Rosch, V. Deckert and J. Popp, *J. Raman Spectrosc.,* 2009, **40**, 1452.
36 T. Deckert-Gaudig, E. Bailo and V. Deckert, *Phys. Chem. Chem. Phys.*, 2009, **11**, 7360.
37 M. Paulite, C. Blum, T. Schmid, L. Opilik, K. Eyer, G. C. Walker and R. Zenobi, *ACS Nano*, 2013, 7, 911.
38 T. Deckert-Gaudig and V. Deckert, *J. Raman Spectrosc.* 2009, **40**, 1446.
39 C. Blum, T. Schmid, L. Opilik, S. Weidmann, S. R. Fagerer and R. Zenobi, *J. Raman Spectrosc*. 2012, **43**, 1895.
40 D. Kurouski, T. Postiglione, T. Deckert-Gaudig, V. Deckert and I. K. Lednev, *Analyst*, 2013, **138**, 1665.
41 E. Podstawka, Y. Ozaki and L. M. Proniewicz, *Appl. Spectrosc.,* 2004, **58**, 570.
42 E. Podstawka, Y. Ozaki and L. M. Proniewicz, *Langmuir*, 2008, **24**, 10807.
43 E. Podstawka-Proniewicz, I. Ignatjev, G. Niaura and L. M. Proniewicz, *J. Phys. Chem. C*, 2012, **116**, 4189.
44 C. Blum, T. Shmid, l. Opilik, N. Metanis, S. Weidmann and R. Zenobi, *J. Phys. Chem. C,* 2012, **116**, 23061.
45 T. Suzuki, T. Itoh, S. Vantasin, S Minami, Y. Kutsuma, K. Ashida, T. Kaneko, Y. Morisawa, T. Miura and Y. Ozaki, *Phys. Chem. Chem. Phys.,* 2014, **16**, 20236.
46 L. E. Hennemann, A. J. Meixner and D. Zhang, *Spectrosc. An. Int. J.,* 2010, **24**, 119.
47 T. Deckert-Gaudig and V. Deckert, *Curr. Opin. Chem. Biol.*, 2011, **15**, 719.
48 S. Vantasin, I. Tanabe, Y. Tanaka, T. Itoh, T. Suzuki, Y. Kutsuma, K. Ashida, T. Kaneko and Y. Ozaki, *J. Phys. Chem. C*, 2014, **118***,* 25809.
49 K. F. Domke and B. Pettinger, *Chem. Phys. Chem.*, 2010, **11**, 1365.
50 B. S. Yeo, E. Amstad, T. Schmid, J. Stadler and R. Zenobi, *Small*, 2009, **5**, 952.
51 A. Creighton, C. G. Blatchford and M. G. Albrecht, *J. Chem. Soc. Farad. Trans. II*, 1979, **75**, 790.
52 A. Savitzky and M. J. E. Goly, *Anal. Chem.* 1964, **36**, 1627.
53 P. Pienpinijtham, E. Proniewicz, Y. Kim, Y. Ozaki, J. R. Lombardi and L. M. Proniewicz, *J. Phys. Chem. C*, 2012, **116**, 16561.
54 K. Faulds, R. E. Littleford, D. Graham, G. Dent and W. E. Smith, *Anal. Chem.*, 2004, **76**, 592.
55 A. E. Aliaga, C. Garrido, P. Leyton, G. Diaz Fleming, J. S. Gomez-Jeria, T. Aguayo, E. Clavijo, M. M. Campos-Vallette and S. Sanchez-Cortes, *Spectrochim. Acta A,* 2010, **76**, 458.
56 J. R. Lombardi and R. L. Birke, *J. Phys. Chem. C,* 2008, **112**, 5605.
57 K. Nakamoto, Infrared and Raman Spectra of Inorganic and Coordination Compounds, 3'rd ed. Wiley, New York, 1978.
58 R. C. Mehrotra and R. Bohra, *Metal Carboxylates*, Academic Press, New York, 1983.
59 Zh. Nickolov, G. Georgiev, D Stoilova and I. Ivanov, *J. Molec. Struct.*, 1995, **354**, 119.
60 S. Deng, H. M. Fan, X. Zhang, K. P. Loh, C-L. Cheng, C. H. Sow and Y. L. Foo, *Nanotechnology*, 2009, **20**, 1.
61 C. Y. Panicker, H. T. Varghese, A. Raj, K. Raju, T. Ertan-Bolelli, I. Yildiz, O. Temiz-Arpacie, C. M. Granadeiro and H. I.S. Nogueira, *Spectrochim. Acta A*, 2009, **74**, 132.
62 V. I. Avdeev and G. M. Zhidomirov, *Surf. Sci.*, 2001, **492**, 137.
63 A. Kudelski, *Chem. Phys. Lett.*, 2006, **427**, 206.
64 A. Kudelski, *Vib. Spectrosc.*, 2006, **41**, 83.
65 D. Pradhan and M. Sharon, *Electrochim. Acta*, 2005, **50**, 2905.
66 C. Pardanaud, C. Martin, P. Roubin, G. Giacometti, C. Hopf, T. Schwarz-Selinger and W. Jacobs, *Diam. Relat. Mater.*, 2013, **34**, 100.